

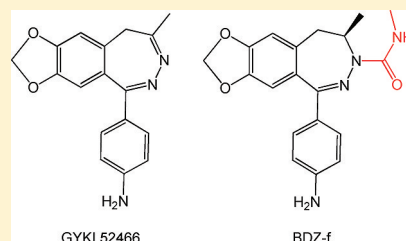
# Mechanism of Inhibition of the GluA2 AMPA Receptor Channel Opening: Consequences of Adding an *N*-3 Methylcarbamoyl Group to the Diazepine Ring of 2,3-Benzodiazepine Derivatives

Congzhou Wang, Zhenyu Sheng,<sup>†</sup> and Li Niu\*

Department of Chemistry, and Center for Neuroscience Research, University at Albany, SUNY, Albany, New York 12222, United States

## S Supporting Information

**ABSTRACT:** 2,3-Benzodiazepine derivatives are AMPA receptor inhibitors, and they are potential drugs for treating some neurological diseases caused by excessive activity of AMPA receptors. Using a laser-pulse photolysis and rapid solution flow techniques, we characterized the mechanism of action of a 2,3-benzodiazepine derivative, termed BDZ-*f*, by measuring its inhibitory effect on the channel-opening and channel-closing rate constants as well as the whole-cell current amplitude of the homomeric GluA2Q AMPA receptor channels. We also investigated whether BDZ-*f* competes with GYKI 52466 for binding to the same site on GluA2Q<sub>flip</sub>. GYKI 52466 is the prototypic 2,3-benzodiazepine compound, and BDZ-*f* is the *N*-3 methylcarbamoyl derivative. We found that BDZ-*f* is a noncompetitive inhibitor with a slight preference for the closed-channel state of both the flip and the flop variants of GluA2Q. Similar to other 2,3-benzodiazepine compounds that we have previously characterized, BDZ-*f* inhibits GluA2Q<sub>flip</sub> by forming an initial, loose intermediate that is partially conducting; however, this intermediate rapidly isomerizes into a tighter, fully inhibitory receptor–inhibitor complex. BDZ-*f* binds to the same noncompetitive site as GYKI 52466 does. Together, our results show that the addition of an *N*-3 methylcarbamoyl group to the diazepine ring with the azomethine feature (i.e., GYKI 52466) is what makes BDZ-*f* more potent and more selective toward the closed-channel conformation than the original GYKI 52466. Our results have useful implications for the structure–activity relationship of the 2,3-benzodiazepine series.



The fundamental postulate of the structure–activity relationship is that molecular activity is a function of its structure; consequently, structurally similar molecules have similar functions. The ultimate goal of studying the structure–activity relationship is to establish predictability for designing better regulatory agents, such as inhibitors, that have higher potency and tighter selectivity toward a common protein target. To achieve such predictability, a set of similar chemical structures is constructed, and rigorous studies, such as the study of the mode of action for these structures, are required to develop atom-based “descriptors” for the structure–activity relationship. For this reason, here we describe a rapid kinetic investigation of the functional consequences of adding an *N*-3 methylcarbamoyl group to the 2,3-benzodiazepine ring as part of our comprehensive study of the structure–activity relationship of 2,3-benzodiazepine compounds.<sup>1,2</sup>

2,3-Benzodiazepine derivatives, also known as GYKI compounds, are synthesized as a group of drug candidates that target  $\alpha$ -amino-3-hydroxy-5-methyl-4-isoxazolepropionic acid (AMPA) receptors. AMPA receptors, together with *N*-methyl-D-aspartate (NMDA) and kainate receptors, belong to the ionotropic glutamate receptor family.<sup>3–5</sup> AMPA receptors mediate most excitatory neurotransmission in the brain and are indispensable for brain development and function, such as memory and learning.<sup>4</sup> However, excessive activity of AMPA receptors leads to extra calcium entry, and the calcium buildup

inside the cell results in cell death.<sup>6,7</sup> This phenomenon, known as excitotoxicity, is a general pathogenic mechanism that underlies several neurological disorders and diseases, including epilepsy, cerebral ischemia, and amyotrophic lateral sclerosis.<sup>4</sup> Thus, compounds that inhibit AMPA receptors, especially those of the GluA2 subunit that control the  $\text{Ca}^{2+}$  permeability,<sup>4,8</sup> are highly sought out as potential drug candidates.

Among different types of AMPA receptor inhibitors, 2,3-benzodiazepine compounds are one of the best because of their tight selectivity for AMPA receptors. Their superior selectivity is due in part to their binding to site(s) distinct from where agonist binds on AMPA receptors.<sup>9,10</sup> Tests of these compounds in animal models also show promising neuroprotection.<sup>10,11</sup> Consequently, hundreds of 2,3-benzodiazepine derivatives have been synthesized based on the prototypic structure of 1-(4-aminophenyl)-4-methyl-7,8-methylenedioxy-5H-2,3-benzodiazepine, also known as GYKI 52466<sup>11</sup> (Figure 1). To make new compounds that are more potent inhibitors, it is important to characterize the structure–activity relationship for existing inhibitors.

To date, the structure–activity relationship for 2,3-benzodiazepine compounds has not been systematically

Received: May 23, 2011

Revised: July 11, 2011

Published: July 13, 2011

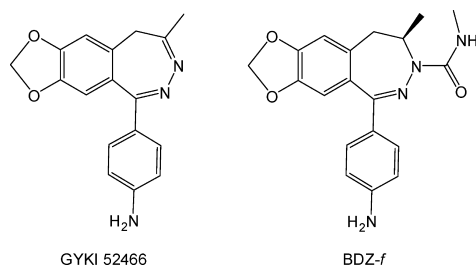


**Figure 1.** Chemical structures of GYKI 52466 and BDZ-f. The chemical names of these compounds are given in the text.

characterized on a time scale comparable to that of the opening of an AMPA receptor channel. AMPA receptors open their channels, in response to the binding of glutamate, the endogenous neurotransmitter, in the microsecond ( $\mu$ s) time scale but desensitize in the millisecond (ms) time domain.<sup>12</sup> Therefore, a kinetic investigation of the mode of action of a 2,3-benzodiazepine compound must be carried out using a technique that provides sufficient time resolution to measure the channel-opening rate of an AMPA receptor.<sup>1</sup> However, commonly used techniques, such as solution flow and single-channel recording, do not have sufficient time resolution for characterizing the effect of a 2,3-benzodiazepine compound on the channel-opening rate process. To overcome that limitation, we used a laser-pulse photolysis technique in this study, together with a photolabile precursor of glutamate or caged glutamate.<sup>13,14</sup> This technique provides a time resolution of  $\sim 60 \mu$ s,<sup>12,14</sup> which is sufficient for measuring the rate of channel opening and for investigating the mechanism of inhibition without the complication of channel desensitization in the millisecond time scale.<sup>1,14</sup>

In this study, we investigated the mechanism by which the GluA2Q<sub>flip</sub> AMPA receptor channel-opening rate process is inhibited by (–)-1-(4-aminophenyl)-4-methyl-7,8-methylenedioxy-4,5-dihydro-3-methylcarbamoyl-2,3-benzodiazepine or BDZ-f (this compound is also named GYKI 53784 or LY 303070; see Figure 1). The questions we asked are the following: What is the mechanism of action of BDZ-f? Does the addition of an N-3 methylcarbamoyl group affect potency and specificity for the open-channel and the closed-channel conformations? Do GYKI 52466 and BDZ-f bind to the same site, or does the addition of an N-3 methylcarbamoyl group affect the binding site? Answers to these questions will allow us to determine whether addition of this group at the N-3 position in the diazepine ring will make BDZ-f a better inhibitor than the parent compound, i.e., GYKI 52466. This report is the third in a comprehensive mechanistic study to establish a more quantitative structure–activity relationship for a series of 2,3-benzodiazepine compounds.<sup>1,2</sup>

## EXPERIMENTAL PROCEDURES

**Cell Culture and Receptor Expression.** Human embryonic kidney (HEK)-293S cells<sup>1</sup> were grown in modified Eagle medium (Invitrogen, Carlsbad, CA) supplemented with 10% fetal bovine serum (Invitrogen), 100 units of penicillin/mL, and 0.1 mg of streptomycin/mL (Sigma-Aldrich, St. Louis, MO). The cells were grown in a humidified incubator at 37 °C and 5% CO<sub>2</sub>. The cells were transfected with the cDNA encoding the rat GluA2Q<sub>flip</sub> receptor subunit<sup>12</sup> by a standard calcium phosphate protocol.<sup>15</sup> For transfection, 4–6  $\mu$ g of the GluA2Q<sub>flip</sub> plasmid was used, together with green fluorescent protein and

simian virus large T-antigen<sup>16</sup> at a ratio of 5:1:0.5. The cells were used 24–48 h later.

**Whole-Cell Current Recording.** Glutamate-induced whole-cell current was recorded on an Axopatch 200B at a cutoff frequency of 2–20 kHz by a built-in, 4-pole low-pass Bessel filter; the whole-cell current traces were digitized at a 5–50 kHz sampling frequency using a Digidata 1322A (Molecular Devices, Sunnyvale, CA). All recordings were collected with transfected HEK-293S cells that were voltage-clamped at –60 mV and 25 °C. pClamp 8 (Molecular Devices) was used for data acquisition. The electrode resistance was  $\sim 3 \text{ M}\Omega$  and filled with the following electrode solution: 110 mM CsF, 30 mM CsCl, 4 mM NaCl, 0.5 mM CaCl<sub>2</sub>, 5 mM EGTA, and 10 mM HEPES (pH 7.4 adjusted by CsOH). The extracellular bath buffer contained 150 mM NaCl, 3 mM KCl, 1 mM CaCl<sub>2</sub>, 1 mM MgCl<sub>2</sub>, and 10 mM HEPES (pH 7.4 adjusted by NaOH). All chemicals used for making buffers were from commercial sources.

**Laser-Pulse Photolysis Measurement.** In the laser-pulse photolysis, we used a caged glutamate or 4-methoxy-7-nitroindolyl-caged-L-glutamate (Tocris Bioscience, Ellisville, MS). We also used  $\gamma$ -O-( $\alpha$ -carboxy-2-nitrobenzyl) glutamate, a different caged glutamate (Invitrogen). A single laser pulse at 355 nm generated from a pulsed Q-switched Nd:YAG laser (Continuum, Santa Clara, CA), with a pulse length of 8 ns and energy output in the range of 200–1000  $\mu$ J, was applied to an HEK-293S cell via optical fiber. Free glutamate solutions were used to calibrate the whole-cell current responses from the same cell before and after a laser flash to estimate the concentration of photolytically released glutamate. A flow device<sup>17,18</sup> was used to deliver free glutamate and/or caged glutamate solutions in the absence and presence of inhibitor and to measure the rate of channel desensitization.<sup>1,18</sup> The device consisted of a U-tube<sup>17</sup> with an aperture of  $\sim 150 \mu$ m. The linear flow rate, controlled by two peristaltic pumps, was 4 cm/s. Once patched, an HEK-293 cell was lifted from the bottom of the dish, suspended in the bath buffer, and placed 50–100  $\mu$ m away from the U-tube aperture.<sup>17,18</sup> The time resolution of this flow device, determined by the rise time of the whole-cell current response (10–90%) to saturating glutamate concentrations, was  $1.0 \pm 0.2$  ms, an average of the measurement from >100 cells expressing the same receptor. For data analysis, the amplitude of the whole-cell current measured by using the flow device was corrected for receptor desensitization as described.<sup>17</sup> Furthermore, we found that full inhibition by BDZ-f was achieved only by preincubating the inhibitor with the GluA2Q<sub>flip</sub> receptor for at least 6 s, similar to what we reported for other 2,3-benzodiazepine compounds.<sup>1</sup> Therefore, in this study, an 8 s preincubation was chosen to ensure the observation of full inhibition. The inhibitor did not activate the GluA2 receptor as the recorded trace did not deviate from the baseline during the preincubation period either when only the inhibitor was exposed to the receptor prior to glutamate application in the flow measurement or when the inhibitor, together with the caged glutamate, was exposed to the receptor prior to a laser pulse in the laser-pulse photolysis measurement.

**Experimental Design and Data Analysis.** BDZ-f was first characterized for its effect on both the channel-opening ( $k_{op}$ ) and the channel-closing ( $k_{cl}$ ) rate processes of the GluA2Q<sub>flip</sub> receptor. Specifically, the effect on  $k_{op}$  and  $k_{cl}$  was determined as a function of inhibitor concentration at two glutamate concentrations by the following rationale. An

observed rate constant ( $k_{\text{obs}}$ ) of GluA2Q<sub>flip</sub> channel opening followed a first-order rate process with or without an inhibitor<sup>1,18</sup> (see eq 1 and all other equations in the Appendix). As shown in eq 2,  $k_{\text{obs}}$  is a function of ligand concentration ( $L$ ), which includes the rate terms of  $k_{\text{op}}$  and  $k_{\text{cl}}$ .<sup>18</sup> When an inhibitor is present, the effect of the inhibitor on, and its inhibition constant for, the open-channel state are determined (eq 4). At a higher ligand concentration, where  $k_{\text{obs}} > k_{\text{cl}}$ , the  $k_{\text{op}}$  value is determined by the difference between  $k_{\text{obs}}$  and  $k_{\text{cl}}$  or by rearranging eq 2 such that  $k_{\text{obs}} - k_{\text{cl}} = k_{\text{op}}[L/(L + K_1)]^2$ . Similarly, the effect of an inhibitor on  $k_{\text{op}}$  and the inhibition constant for the closed-channel state are determined (eq 5). We have previously established the criteria by which  $k_{\text{cl}}$  can be determined from the measurement of  $k_{\text{obs}}$ .<sup>1,12,18</sup> For GluA2Q<sub>flip</sub> specifically,  $k_{\text{cl}}$  is numerically equal to the  $k_{\text{obs}}$  value obtained at a glutamate concentration of 100  $\mu\text{M}$ , which corresponds to  $\sim 4\%$  of the fraction of the open-channel form.<sup>1,12,18</sup> In this study, therefore, the effect of BDZ-f on  $k_{\text{cl}}$  was determined at a glutamate concentration of 100  $\mu\text{M}$ .<sup>1</sup> The effect of BDZ-f on  $k_{\text{op}}$  was determined at a glutamate concentration of 300  $\mu\text{M}$ .<sup>1</sup> At this concentration the difference between  $k_{\text{op}}$  and  $k_{\text{cl}}$  could be detected while the energy used for laser photolysis was still well tolerated by the cell.

The effect of BDZ-f on the whole-cell current amplitude ( $A$ ) was measured to independently determine an inhibition constant. Specifically, we used a low glutamate concentration (i.e.,  $L \ll K_1$ ), at which most receptors were in the closed-channel state (see Figure 4; defined as the unliganded, singly and doubly liganded forms), to determine the inhibition constant for the closed-channel state according to eqs 6a and 6b. Conversely, we used a saturating ligand ( $L \gg K_1$ ), where most of the receptors were in the open-channel state, to determine the inhibition constant for the open-channel state.<sup>1</sup> For GluA2 receptors, we chose 100  $\mu\text{M}$  and 3 mM glutamate concentrations, which correspond to  $\sim 4\%$  and  $\sim 95\%$  of the open-channel form, respectively.<sup>1</sup>

We also examined the effect of two inhibitors, i.e., BDZ-f and GYKI 52466, on the whole-cell current amplitude. This double-inhibitor experiment was designed to test whether both inhibitors bound to the same site on the receptor. In this experiment, the concentration of one inhibitor was kept constant while the concentration of the other was varied. An apparent inhibition constant obtained from the two-inhibitor experiment (or the slope of the  $A/A_{\text{I,P}}$  plot; see eqs 7 and 8) was compared to that obtained from one-inhibitor experiment (or the slope of the  $A/A_1$  plot; see eqs 6a and 6b). All other conditions were the same as described before.

Origin 7 (Origin Lab, Northampton, MA) was used for both linear and nonlinear regressions (Levenberg–Marquardt and simplex algorithms). Unless otherwise noted, each data point shown in a plot was an average of at least three measurements collected from at least three cells. The error reported refers to the standard deviation of a fit.

## RESULTS

**BDZ-f Inhibited the Channel-Opening Process of GluA2Q<sub>flip</sub>.** Using the laser-pulse photolysis technique, we characterized the effect of BDZ-f on the channel-opening rate

process of GluA2Q<sub>flip</sub>. As shown in a pair of representative whole-cell recording traces initiated by laser-pulse photolysis of the caged glutamate (Figure 2A), the current rise was slowed

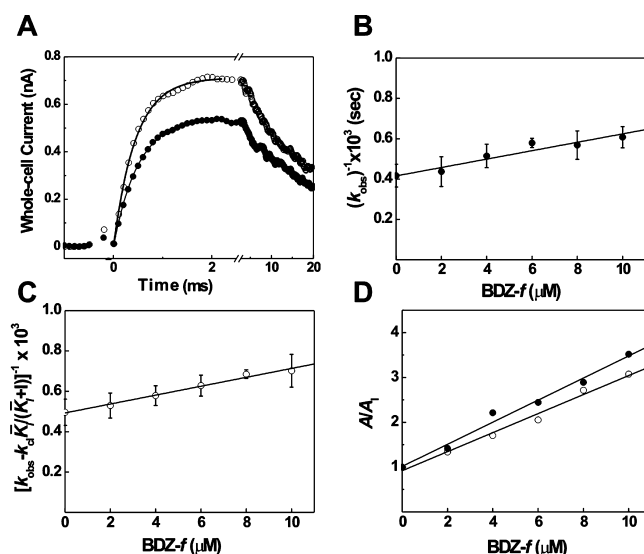


**Figure 2.** (A) Representative whole-cell traces from the laser-pulse photolysis experiment showing that BDZ-f inhibited both the rate and the amplitude of the opening of the GluA2Q<sub>flip</sub> channels. The whole-cell current amplitude was measured in the absence and presence of BDZ-f. The top trace ( $\circ$ ) is the control ( $k_{\text{obs}} = 2439 \text{ s}^{-1}$ ;  $A = 0.74 \text{ nA}$ ), and the lower one ( $\bullet$ ) was recorded with 2  $\mu\text{M}$  BDZ-f ( $k_{\text{obs}} = 1988 \text{ s}^{-1}$ ;  $A = 0.53 \text{ nA}$ ). The concentration of the photolytically released glutamate was estimated to be  $\sim 100 \mu\text{M}$  in both cases. (B) Effect of BDZ-f on  $k_{\text{cl}}$  obtained at 100  $\mu\text{M}$  of photolytically released glutamate and as a function of BDZ-f concentration. A  $K_1$  of  $20 \pm 3 \mu\text{M}$  was determined using eq 4. (C) Effect of BDZ-f on  $k_{\text{op}}$  obtained at 300  $\mu\text{M}$  of photolytically released glutamate and as a function of BDZ-f concentration. A  $K_1$  of  $22 \pm 1 \mu\text{M}$  was determined using eq 5. (D) Effect of BDZ-f on the whole-cell current amplitude of GluA2Q<sub>flip</sub> receptors obtained from the laser-pulse photolysis measurement. Using eq 6a, a  $K_1$  of  $4.0 \pm 0.2 \mu\text{M}$  was determined at 100  $\mu\text{M}$  of photolytically released glutamate ( $\bullet$ ); a  $K_1$  of  $4.7 \pm 0.3 \mu\text{M}$  was obtained at 300  $\mu\text{M}$  of photolytically released glutamate ( $\circ$ ).

and the current amplitude was reduced in the presence of BDZ-f, indicating that BDZ-f inhibited the opening of the GluA2Q<sub>flip</sub> receptor channel. The observed rate constant in the absence ( $k_{\text{obs}}$ ) and presence of an inhibitor ( $k_{\text{obs}}'$ ) followed a first-order rate process for over 95% of the rising phase (i.e., the solid lines in Figure 2A). This kinetic feature was observed without exception in all inhibitor and glutamate concentrations used, not only in this study but also in our earlier studies of GluA2Q<sub>flip</sub> in the absence<sup>12</sup> and presence of other inhibitors.<sup>1,2</sup> These results were therefore consistent with the notion that the rate of the current rise in the laser-pulse photolysis measurement was pertinent to the channel-opening rate, and the reduction of the rate of the current rise was ascribed to the inhibition of the channel opening by an inhibitor,<sup>1,2</sup> such as BDZ-f.

To investigate the mechanism of inhibition, we characterized the effect of BDZ-f on both  $k_{\text{op}}$  and  $k_{\text{cl}}$ .<sup>1,2</sup> Specifically, at the 100  $\mu\text{M}$  glutamate concentration where  $k_{\text{cl}}$  was measured (see Experimental Procedures),  $K_1$ , the inhibition constant for the open-channel state, was found to be  $20 \pm 3 \mu\text{M}$  for BDZ-f (Figure 2B). At the 300  $\mu\text{M}$  glutamate concentration, where  $k_{\text{obs}} > k_{\text{cl}}$  and thus  $k_{\text{op}}$  was measurable,  $K_1$ , the inhibition

**Table 1. Inhibition Constants of BDZ-f Obtained from Rate and Amplitude Measurements for the Closed- and Open-Channel States of GluA2Q<sub>flip</sub>**

inhibitor	rate measurement <sup>a</sup>		amplitude measurement			
	$K_i$ ( $\mu\text{M}$ ) <sup>b,d</sup> (closed channel)	$\bar{K}_i$ ( $\mu\text{M}$ ) <sup>b,e</sup> (open channel)	$K_i$ ( $\mu\text{M}$ ) <sup>b,d</sup>	$K_i$ ( $\mu\text{M}$ ) <sup>b,e</sup>	$K_i$ ( $\mu\text{M}$ ) <sup>c,d</sup> (closed channel)	$\bar{K}_i$ ( $\mu\text{M}$ ) <sup>c,f</sup> (open channel)
BDZ-f	22 ± 1	20 ± 3	4.0 ± 0.2	4.7 ± 0.3	3.8 ± 0.4	5.4 ± 0.8
GYKI 52466 <sup>g</sup>	61 ± 11	128 ± 30	15 ± 1	16 ± 1	14 ± 1	30 ± 2
BDZ-3 <sup>h</sup>	514 ± 60	204 ± 18	200 ± 18	69 ± 4	210 ± 20	38 ± 10

<sup>a</sup>The constants obtained from rate measurements represent those in the first step of inhibition as in Figure 4, whereas those obtained from the amplitude measurements represent the overall inhibition constants. <sup>b</sup>Laser-pulse photolysis measurement. <sup>c</sup>Flow measurement. <sup>d</sup>Measurements at 100  $\mu\text{M}$  glutamate for the closed-channel state. <sup>e</sup>Measurements at  $\sim 300$   $\mu\text{M}$  glutamate. <sup>f</sup>Measurements at 3 mM glutamate. <sup>g</sup>Ritz et al. (2011), in press. <sup>h</sup>Ritz et al., 2008.

constant for the closed-channel state, was  $22 \pm 1$   $\mu\text{M}$  (Figure 2C). The fact that BDZ-f inhibited both  $k_{\text{cl}}$  and  $k_{\text{op}}$  was consistent with it being a noncompetitive inhibitor. In contrast, an uncompetitive inhibitor would be expected to inhibit only  $k_{\text{cl}}$  but not  $k_{\text{op}}$ , whereas a competitive inhibitor would be expected to inhibit  $k_{\text{op}}$  but not  $k_{\text{cl}}$ .<sup>1,2</sup>

**Effect of BDZ-f on the Amplitude of Whole-Cell Current Observed in the Laser-Pulse Photolysis Measurement.** In the measurement of laser-pulse photolysis (Figure 2A), BDZ-f also inhibited the amplitude of the whole-cell current response. The magnitude of the reduction in current amplitude was also used to estimate an inhibition constant by eqs 6a and 6b. From the ratio of the current amplitude in the absence of BDZ-f to the amplitude in presence of BDZ-f (Figure 2D), we found a  $K_i$  of  $4.0 \pm 0.2$   $\mu\text{M}$  for the closed-channel state (i.e., at 100  $\mu\text{M}$  glutamate as in Figure 2D, solid circles; see also Experimental Procedures and eqs 6a, 6b). Similarly, a  $K_i$  of  $4.7 \pm 0.3$   $\mu\text{M}$  was estimated at 300  $\mu\text{M}$  glutamate (Figure 2D, open circles). All the inhibition constants obtained from the laser photolysis measurement (and solution flow measurement, described in detail below) are summarized in Table 1.

We compared the magnitude of the inhibition constants obtained from the rate with those obtained from the amplitude but found that the inhibition constants calculated from the amplitude were about 5-fold smaller than those calculated from the rate, even from the same measurement, i.e., the laser-pulse photolysis experiment (Figure 2A). To make sure that this discrepancy between the corresponding inhibition constants determined from the amplitude and rate measurements was real, we further evaluated the inhibition constants using a solution flow technique (see Experimental Procedures). The flow measurement using free glutamate concentrations served as the control to determine an inhibition constant from the amplitude of whole-cell current in the absence and presence of BDZ-f.

**Effect of BDZ-f on the Amplitude of Whole-Cell Current Observed in the Flow Measurement.** As shown in glutamate-evoked whole-cell current traces in the absence (left trace of Figure 3A) and presence (right trace) of BDZ-f in the solution flow measurement, BDZ-f inhibited the current amplitude from the GluA2Q<sub>flip</sub> receptor channels. By setting glutamate concentrations to be 100  $\mu\text{M}$  and 3 mM<sup>1</sup> (see Experimental Procedures), we determined that the  $K_i$  was  $3.8 \pm 0.4$   $\mu\text{M}$  for the closed-channel and  $\bar{K}_i$  was  $5.4 \pm 0.8$   $\mu\text{M}$  for the open-channel state (these values are also summarized in Table 1).

On the basis of these results, we conclude the following: (i) That BDZ-f inhibited the whole-cell current response from

both the closed-channel and the open-channel states of GluA2Q<sub>flip</sub> was consistent with its effect on the rate of channel opening, again suggesting that BDZ-f inhibited the GluA2Q<sub>flip</sub> channel in a noncompetitive fashion. (ii) Quantitatively, the  $K_i$  values for BDZ-f calculated from the amplitude data for the closed-channel state were similar (3.8  $\mu\text{M}$  vs 4  $\mu\text{M}$  from the flow and laser experiments, respectively; Table 1). (iii) The  $\bar{K}_i$  value of BDZ-f for the open-channel state was slightly higher than the value for the closed-channel state (5.4  $\mu\text{M}$  vs 3.8  $\mu\text{M}$ , respectively; Table 1), suggesting that BDZ-f was slightly more selective for the closed-channel state. (iv) The inhibition constant obtained from the amplitude data (4.7  $\mu\text{M}$ ) collected from the laser experiment at 300  $\mu\text{M}$  of glutamate was within this range (i.e.,  $3.8 < 4.7 < 5.4$   $\mu\text{M}$ ; see Table 1). This was expected because the fraction of the open-channel form that corresponded to 300  $\mu\text{M}$  was 10%, which was within the range of 4%–95% (or 100  $\mu\text{M}$ –3 mM glutamate).

To calculate the inhibition constants from the current amplitude obtained from the solution flow experiments, we used the total amplitude of the current response in the absence and presence of BDZ-f (Figure 3B). However, we also examined an entire whole-cell current trace that included both the desensitizing and nondesensitizing or steady-state phase (Figure 3A,D). First, we found that BDZ-f did not affect the desensitization rate constant ( $k_{\text{des}}$ , in Figure 3C). As shown here (see the upper and lower hollow symbols in Figure 3C) and previously,<sup>12</sup>  $k_{\text{des}}$  was dependent only on ligand concentration yet was independent of inhibitor concentration (up to 10  $\mu\text{M}$ , the highest concentration used in this study). This result indicated that BDZ-f reduced the current amplitude by inhibiting the open channel through which the current was generated but did not affect the rate by which the channel desensitized. Second, the desensitization of the GluA2Q<sub>flip</sub> channels proceeded in two phases, i.e., a rapidly desensitizing phase (the major phase, whose rate constants are shown in Figure 3C) and a nondesensitizing phase (the minor phase, an example is shown in Figure 3D). The fraction of the nondesensitizing phase was glutamate-concentration-dependent in that at a glutamate concentration of 100  $\mu\text{M}$  the percentage of the nondesensitizing phase was  $\sim 18\%$ , and at a glutamate concentration of 3 mM it was only  $\sim 2\%$  (based on the measurement of 55 and 49 cells, respectively). In addition, the absolute current amplitude of the nondesensitizing phase, collected from the same cell and at these two glutamate concentrations, seemed to be only slightly changed; however, the absolute amplitude of the nondesensitizing phase observed at either glutamate concentration was small (Table S1 in Supporting Information). A similar percentage of the nondesensitizing phase for other AMPA receptor subunits but at saturating glutamate concentration,

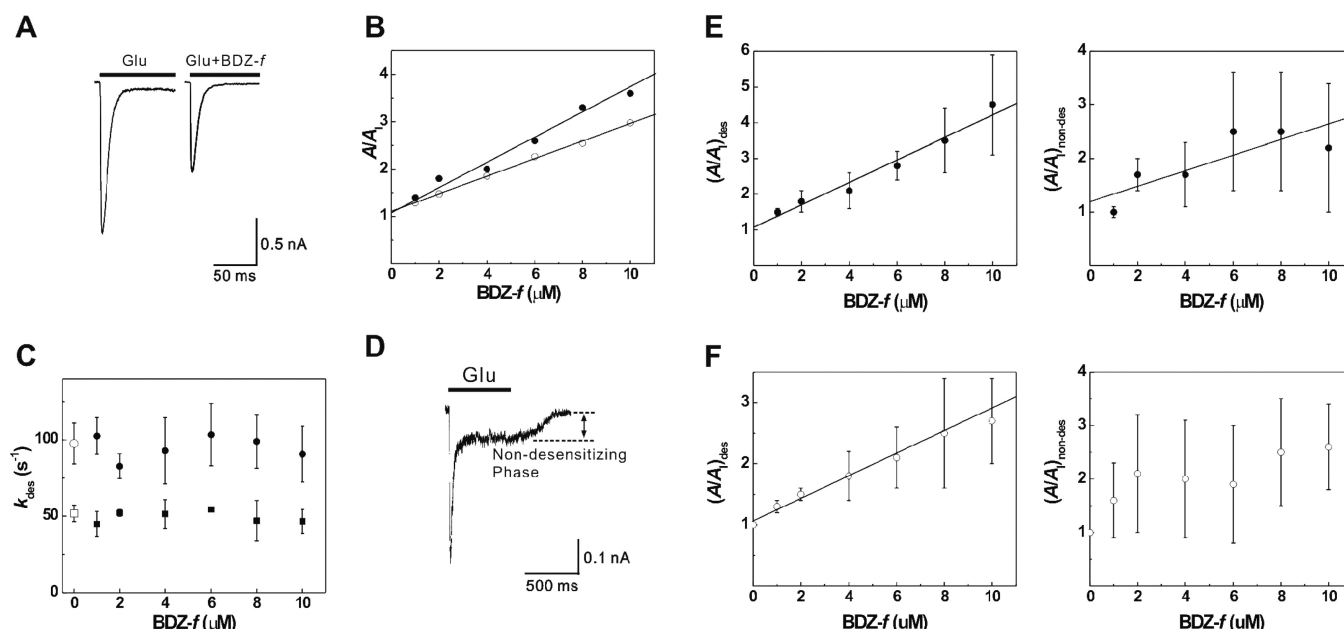


**Figure 3.** (A) Representative whole-cell currents mediated by GluA2Q<sub>flip</sub> receptors expressed in HEK-293S cells in the absence (left) and presence (right) of BDZ-f, obtained by flow measurement. The concentrations of glutamate and BDZ-f are 3 mM and 2  $\mu\text{M}$ , respectively. The inhibition ratio ( $A/A_1$ ) for the pair is  $\sim 1.61$ . The whole-cell current was recorded at  $-60$  mV, pH 7.4, and 22  $^{\circ}\text{C}$ . (B) Effect of BDZ-f on the whole-cell current amplitude of GluA2Q<sub>flip</sub> receptors obtained from the flow measurement.  $K_1$  of  $3.8 \pm 0.4$   $\mu\text{M}$  was determined by using eqs 6a and 6b for the closed-channel state (100  $\mu\text{M}$  glutamate,  $\bullet$ );  $\bar{K}_1$  of  $5.4 \pm 0.8$   $\mu\text{M}$  was obtained for the open-channel state (3 mM glutamate,  $\circ$ ). (C) Effect of BDZ-f on the channel desensitization rates for the closed-channel (lower, determined at 100  $\mu\text{M}$  glutamate) and open-channel (upper, determined at 3 mM glutamate) states of GluA2Q<sub>flip</sub>. (D) A representative whole-cell current mediated by GluA2Q<sub>flip</sub> receptors at 100  $\mu\text{M}$  of glutamate shows that the total current amplitude ( $A_{\text{tot}}$ ) equals 425 pA with the amplitude of nondesensitizing phase ( $A_{\text{non-des}}$ ) remaining at 61 pA (until glutamate was removed) and the desensitizing phase being 364 pA. The fraction of the nondesensitizing phase is 14%. (E) Effect of BDZ-f on the two components of the whole-cell current for the closed-channel state of GluA2Q<sub>flip</sub> receptors. In the left panel, the amplitude of the desensitized phase is plotted against inhibitor concentration, and a  $K_1$  of  $3.2 \pm 0.3$   $\mu\text{M}$  was determined. In the right panel, a  $K_1$  of  $6.9 \pm 2.3$   $\mu\text{M}$  was determined for the nondesensitizing phase. (F) Effect of BDZ-f on the two components of the whole-cell current for the open-channel conformation of GluA2Q<sub>flip</sub>. In the left panel, the amplitude of the desensitized phase is plotted against inhibitor concentration, and a  $\bar{K}_1$  of  $5.4 \pm 0.3$   $\mu\text{M}$  was determined. We did not estimate an inhibition constant for the data on the right panel due to large experimental error.

ranging from 0.6% to 2.4%, has been documented (see a review in ref 4). It should be noted that the percentage of the nondesensitizing phase in GluA2, as we described here, is for the flip variant of GluA2Q, one of the two alternatively spliced isoforms of GluA2.<sup>19</sup> The flop variant desensitizes almost completely.<sup>19–21</sup> The nondesensitizing phase is thought to link to the firing of action potential from AMPA-containing neurons and the propagation of action potential in postsynapses.<sup>22</sup> Furthermore, it is thought that a sustained existence of the nondesensitizing phase, due to prolonged low-level glutamate exposure, causes cell death.<sup>23</sup>

On the basis of the analysis described above, we separately examined the effect of BDZ-f on the current amplitude of the desensitizing and the nondesensitizing phases. For the closed-channel form, we obtained  $K_1$  of  $3.2 \pm 0.3$   $\mu\text{M}$  from the desensitizing phase (Figure 3E, left panel) and  $K_1$  of  $6.9 \pm 2.3$   $\mu\text{M}$  from the nondesensitizing phase (Figure 3E, right panel). Conversely, for the open-channel form or at 3 mM glutamate concentration, we calculated  $\bar{K}_1$  to be  $5.4 \pm 0.3$   $\mu\text{M}$  from the desensitizing phase (Figure 3F, left panel). However, we could not estimate a statistically significant inhibition constant from the nondesensitizing phase (Figure 3F, right panel) because of a large experimental error range. We then compared the inhibition constants from the fractional amplitude with those from the total amplitude. We found that for the open-channel state  $\bar{K}_1$  of 5.4  $\mu\text{M}$  calculated from the fractional amplitude (i.e., the desensitizing phase only) was identical to  $\bar{K}_1$  of 5.4  $\mu\text{M}$

from the total amplitude. This was not surprising because at a high glutamate concentration, where the effect of BDZ-f on the open-channel form was measured, the desensitizing phase dominated the total current amplitude. At a low glutamate concentration, where the desensitizing phase became relatively less dominant and the nondesensitizing phase became relatively more significant,  $K_1$  of  $3.2 \pm 0.3$   $\mu\text{M}$  from the desensitizing phase was identical to the  $K_1$  value ( $3.8 \pm 0.4$   $\mu\text{M}$ ) calculated from the total amplitude. Therefore, these comparisons suggest that the use of the total current amplitude is reliable enough for estimating the inhibition constants for both the open-channel and closed-channel states.

**BDZ-f Inhibits Channel Opening by a Two-Step Process.** That BDZ-f inhibited  $k_{\text{cl}}$  and  $k_{\text{op}}$  as well as the whole-cell current amplitude at both high and low glutamate concentrations, which reflected the open-channel and closed-channel states, respectively, is consistent with a noncompetitive mechanism of inhibition. Quantitatively, the inhibition constants determined from the amplitude ratio from both the laser and flow measurements were in good agreement (Table 1). Those constants, however, were  $\sim 5$ -fold smaller than the inhibition constants determined from the measurement of the channel-opening rate. The discrepancy between these inhibition constants and all other pieces of mechanistic evidence we obtained from this study led us to establish a minimal mechanism of inhibition for BDZ-f (Figure 4), i.e., the same mechanism we have proposed for other 2,3-benzodiazepine

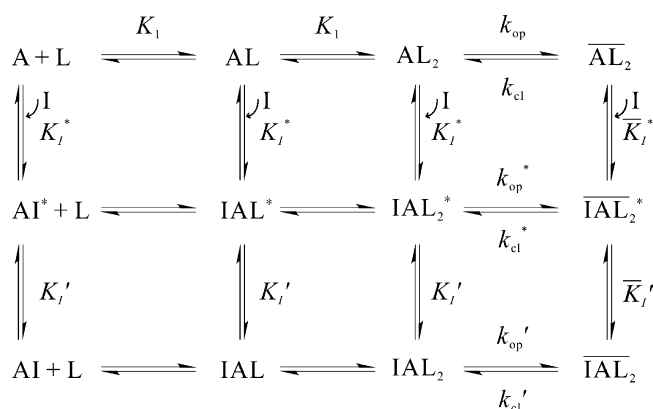


**Figure 4.** A minimal mechanism of inhibition for BDZ-*f*. The upper row shows the channel-opening reaction of the AMPA receptor. A represents the active, unliganded form of the receptor, L the ligand (glutamate), AL and AL<sub>2</sub> the ligand-bound closed-channel forms,  $\overline{AL}_2$  the open-channel state of the receptor (all the species with a bar sign refer to open-channel state),  $k_{op}$  the channel-opening rate constant, and  $k_{cl}$  the channel-closing rate constant. For simplicity and without contrary evidence, it is assumed that glutamate binds to the two steps with equal affinity, represented by the same intrinsic equilibrium dissociation constant,  $K_1$ . The initial binding of BDZ-*f* to the receptor is assumed to form a loosely bound, partially conducting intermediate (e.g.,  $\overline{IAL}_2^*$ ) in both the closed-channel and open-channel states of the receptor (middle to the lower row), the receptor:inhibitor intermediate rapidly isomerizes into a more tightly bound complex ( $\overline{IAL}_2$ ), and such a complex is no longer capable of conducting ions. The inhibition constants pertinent to various steps in this mechanistic scheme are shown in Table 1.  $K_1$  represents the overall inhibition constant associated with the closed-channel state of the receptor (i.e., the values from column 5 in Table 1),  $\overline{K}_1$  the overall inhibition constant associated with open-channel state (i.e., the values from column 6 in Table 1), I the inhibitor,  $k_{op}'$  the channel-opening rate constant of the inhibited AMPA receptor, and  $k_{cl}'$  the channel-closing rate constant of the inhibited AMPA receptor. In addition, the values for  $K_1^*$  and  $\overline{K}_1^*$  for step 1 can be also found from columns 1 and 2 in Table 1.

inhibitors of AMPA receptors.<sup>1,2</sup> By this mechanism, the initial binding of BDZ-*f* to the receptor is assumed to form a loosely bound intermediate (e.g.,  $\overline{IAL}_2^*$ ) in both the closed-channel and open-channel states of the receptor. A receptor:inhibitor intermediate is partially conducting, which yields partial inhibition of channel activity. In the second step, the receptor:inhibitor intermediate rapidly isomerizes into a more tightly bound complex ( $\overline{IAL}_2$ ), and such a complex is no longer capable of conducting ions.

The proposed mechanism of inhibition (Figure 4) is plausible because it can account for the results we obtained for BDZ-*f*. First, both the rate and the amplitude measurements in the laser-pulse photolysis experiment with BDZ-*f* (as in Figure 2A) were associated with the channel-opening process. Amplitude, however, was an equilibrium measure (the channel-opening equilibrium is transient because the channel becomes desensitized in the millisecond time scale). Thus, a stronger inhibition or a smaller  $K_1$  value calculated from the amplitude suggested that a larger inhibition constant or a less than full inhibition obtained from the rate in the same experiment, i.e., the photolysis-triggered whole-cell traces (Figure 2A), reflected only a fraction of the overall inhibition. In other words, the effect of BDZ-*f* on the channel-opening rate was only partial; full inhibition would have to be produced from an additional

step, i.e., the isomerization reaction, which turned the initial, partially conducting complex into a totally inhibiting complex. As such, only one step or the slow step in the mechanism was observable in the rate measurement. It should be noted that eqs 4 and 5 were derived based on a one-step process, and those equations allowed us to estimate the inhibition constants (Table 1) associated with the slow step, which limited the observed rate of the reaction in the presence of the inhibitor.

Evidence from this study suggested that the first step in the minimal mechanism of inhibition was the slow step (Figure 4) or the step in which the loose receptor:inhibitor intermediates are formed in the closed- and open-channel states. The assumption that the first step is slow compared with the second step was based on the observation that throughout the concentration range for both glutamate and inhibitor only a single-exponential rise for the opening of the channel was observed. If the rate of the second step was slow or comparable to that of the first step, we would expect complete or nearly complete inhibition because the inhibition constants calculated from the rate data would agree fully or nearly fully with those from the amplitude. Furthermore, the fact that  $1/k_{obs}$  increased linearly with increasing inhibitor concentration as predicted by eqs 4 and 5 (Figure 2B,C) in both the closed-channel and open-channel states of the receptor further supports the notion that the rate of the isomerization reaction from both the closed-channel and open-channel pathways (Figure 4) would have to be faster than the initial step. Consequently, the  $\overline{K}_1^*$  value (Table 1) obtained from the rate measurement at a high glutamate concentration was thought to be pertinent to the inhibition of the open channel by the initial inhibitor:receptor intermediate, whereas the  $K_1^*$  value (Table 1) was assigned to the inhibition of the closed-channel state by the initial inhibitor:receptor intermediate (Table 1).

Although the effect of BDZ-*f* on both  $k_{op}$  and  $k_{cl}$  was partial, which we determined from the rate of channel opening in the absence and presence of the inhibitor (Table 1), that BDZ-*f* inhibited both  $k_{op}$  and  $k_{cl}$  was consistent with its acting in a noncompetitive mechanism and inconsistent with either a competitive or an uncompetitive mechanism of inhibition. By a competitive mechanism, BDZ-*f* would compete with glutamate for the same binding site. Consequently, only the effect on  $k_{op}$ , but not on  $k_{cl}$ , would be expected. In other words, there would be no  $[\overline{K}_1/(\overline{K}_1 + I)]$  term associated with  $k_{cl}$  in eq 3, and thus  $1/k_{obs}$ , as in eq 4, would be independent of inhibitor concentration. By an uncompetitive mechanism, commonly known as an open-channel blockade, BDZ-*f* would inhibit the open-channel state only; i.e., only the effect on  $k_{cl}$ , but not on  $k_{op}$ , would be expected. In this scenario, the  $[K_1/(K_1 + I)]$  term associated with  $k_{op}$  in eq 3 would not exist. Consequently, the  $(k_{obs} - k_{cl}')$  term, as in eq 5, would not be dependent on inhibitor concentration.

**BDZ-*f* Inhibited Almost Equally Strongly the Closed-Channel and Open-Channel States of Both the Flip and Flop Variants of GluA2Q.** On the basis of the overall inhibition constants (Table 1), we conclude that BDZ-*f* inhibited both the closed-channel and open-channel states of GluA2Q<sub>flip</sub> receptors roughly equally, although there was a slight preference for the closed-channel state over the open-channel state, i.e.,  $K_1$  of  $3.8 \pm 0.4 \mu\text{M}$  vs  $\overline{K}_1$  of  $5.4 \pm 0.8 \mu\text{M}$ , respectively. Thus far, the studies that led to these conclusions were carried out with the flip variant of GluA2Q (or precisely GluA2Q<sub>flip</sub> receptors). However, these data raise two

interesting questions. First, does BDZ-*f* show a similar potency and selectivity for the flop variant of GluA2Q? The flip and the flop variants are generated by alternative splicing, and GluA2Q<sub>flip</sub> and GluA2Q<sub>flop</sub> have only nine different amino acids.<sup>19</sup> However, the homomeric channels assembled from the flip and flop variants of GluA2Q have different kinetic properties, such that GluA2Q<sub>flop</sub> has the same  $k_{op}$  but a larger  $k_{cl}$  than the flip variant.<sup>24</sup> Using the flow technique, we measured the overall inhibition constants for the closed- and open-channel states of the receptor. We found that BDZ-*f* had a similar inhibitory property on the flop variant as it did on the flip variant. Specifically, BDZ-*f* inhibited the GluA2Q<sub>flop</sub> receptors expressed in HEK-293 cells with a  $K_I$  of  $3.8 \pm 0.3 \mu\text{M}$  for the closed-channel state and a  $\bar{K}_I$  of  $5.6 \pm 0.6 \mu\text{M}$  for the open-channel state (Figure 5). These inhibition

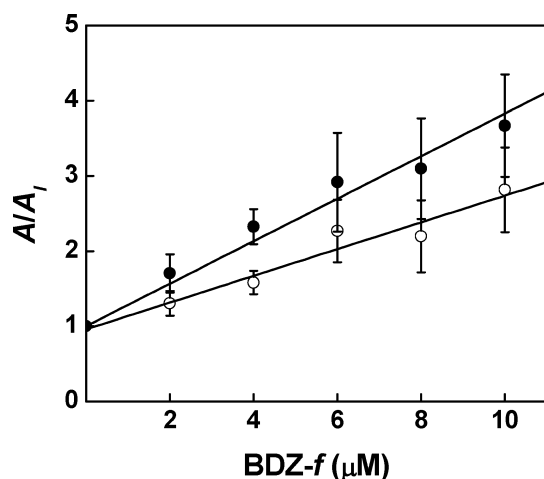


**Figure 5.** Effect of BDZ-*f* on the whole-cell current amplitude of the GluA2Q<sub>flop</sub> receptors obtained from the flow measurement. The inhibition constants were determined from this plot by using eqs 6a and 6b.  $K_I$  of  $3.8 \pm 0.3 \mu\text{M}$  was determined for the closed-channel state (100  $\mu\text{M}$  glutamate, ●); a  $\bar{K}_I$  of  $5.6 \pm 0.6 \mu\text{M}$  was obtained for the open-channel state (3 mM glutamate, ○).

constants were similar to those for GluA2Q<sub>flip</sub> (Table 1). Therefore, we conclude that BDZ-*f* is equally effective on the flop variant of the same receptor but had a slight preference for the closed-channel state of the flop receptor. Because BDZ-*f* did not show any preference in potency between the two alternatively spliced variants and yet the flip/flop sequence segments differ by nine amino acids, it is unlikely that the flip/flop sequence segment of GluA2 is involved critically in making up the noncompetitive site on GluA2.

**BDZ-*f* and GYKI 52466 Bind to the Same Site on GluA2Q<sub>flip</sub>.** Next we investigated whether BDZ-*f* binds to the same site as GYKI 52466 does. Whether a slight modification of a structure is enough to change the binding site for the new compound is one of the essential questions in defining the structure–activity relationship. We previously hypothesized that the 2,3-benzodiazepine compounds with the azomethine group on the diazepine ring, which contains the 4-methyl group (see Figure 1), bind to the same site, whereas 2,3-benzodiazepine compounds with an  $\epsilon$ -lactam structure, which contains the 4-carbonyl group, bind to a different site.<sup>2</sup> Therefore, BDZ-*f* and GYKI 52466 were expected to compete for binding to the same site, given that BDZ-*f* and GYKI 52466 share the same

4-methyl group, although BDZ-*f* contains an extra *N*-3 methylcarbamoyl group (Figure 1). To investigate this question, we performed a double-inhibitor experiment (see details in Experimental Procedures). Specifically, GYKI 52466 and BDZ-*f* were applied concurrently to the closed-channel state of the GluA2Q<sub>flip</sub> receptor in that the concentration of GYKI 52466 was fixed while the concentration of BDZ-*f* was varied (Figure 6A). We found that the double-inhibition constant,

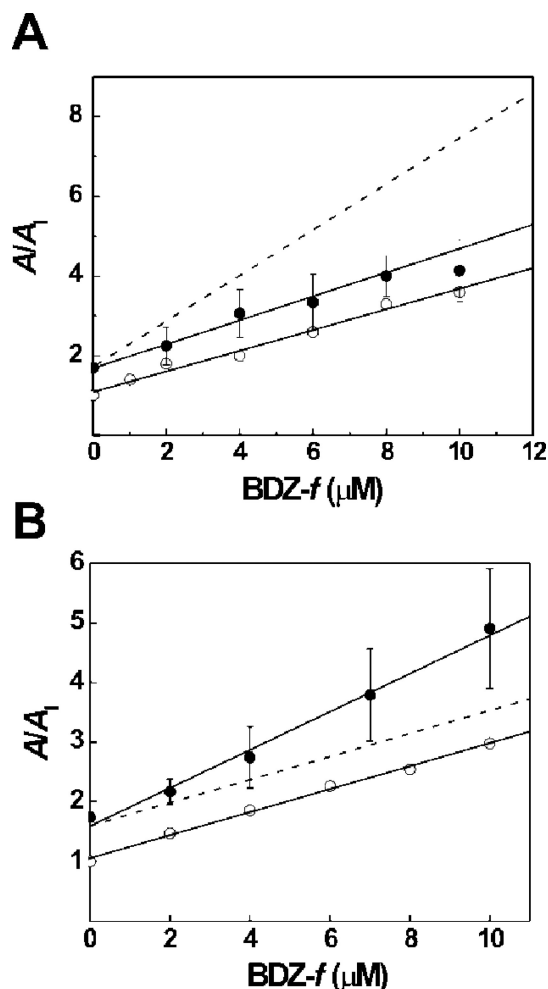


**Figure 6.** (A) The result of a double-inhibition experiment for GYKI 52466 and BDZ-*f* on GluA2Q<sub>flip</sub> determined at 100  $\mu\text{M}$  glutamate concentration. The concentration of GYKI 52466 was fixed at 15  $\mu\text{M}$ . The double-inhibition constant,  $K'_I$ , was determined to be  $3.6 \pm 0.6 \mu\text{M}$  (filled circles), compared with  $K_I$  of  $3.8 \pm 0.4 \mu\text{M}$  for BDZ-*f* alone (open circles). The dashed line simulates the  $A/A_1$  ratio by using eq 8, assuming that the two inhibitors bind to two different sites with a double-inhibition constant of  $\sim 1.9 \mu\text{M}$  (when GYKI 52466 was fixed at 15  $\mu\text{M}$ ). (B) The result of the double-inhibition experiment for BDZ-2 and BDZ-*f* on GluA2Q<sub>flip</sub> determined at 3 mM glutamate concentration. The double-inhibition constant,  $\bar{K}'_I$ , was determined to be  $3.1 \pm 0.2 \mu\text{M}$  (filled circles) compared with  $\bar{K}_I$  of  $5.4 \pm 0.8 \mu\text{M}$  for BDZ-*f* alone (open circles). The dashed line represents the simulated  $A/A_1$  values by using eq 7, assuming that the two inhibitors bind to the same site with an inhibition constant of  $\sim 5.4 \mu\text{M}$  (when BDZ-2 was fixed at 8  $\mu\text{M}$ ).

$K'_I = 3.6 \pm 0.6 \mu\text{M}$ , was identical to  $K_I = 3.8 \pm 0.4 \mu\text{M}$  for BDZ-*f* alone (Figure 3B and Table 1), indicating that the two inhibitors competed for the same binding site on the GluA2Q<sub>flip</sub> receptor. If GYKI 52466 and BDZ-*f* bound to two different

noncompetitive sites on the same receptor, a much stronger inhibition would have been expected (Figure 6A, dashed line simulated by eq 8). This was because the concentration of two inhibitors, each binding to its own site independently, would have been higher, thus producing stronger inhibition. We performed another double-inhibitor experiment with BDZ-*f* and 1-(4-aminophenyl)-3,5-dihydro-7,8-methylenedioxy-4*H*-2,3-benzodiazepin-4-one (BDZ-2) (Figure S1 in the Supporting Information). BDZ-2 has a 4-carbonyl group on the diazepine ring or, precisely, a  $\epsilon$ -lactam structure. Thus, as a control, we expected that BDZ-2 and BDZ-*f* would bind to two separate sites. In fact, that was exactly what we found (Figure 6B). A larger slope was expected when both inhibitors were present because the collective inhibition was attributed to two sites. The dashed line in Figure 6B shows the simulation of a one-site binding/inhibition by the use of eq 7.

## DISCUSSION

In the present study, we characterized the mechanism of action of BDZ-*f* by measuring its inhibitory effect on the channel-opening and channel-closing rate constants as well as the whole-cell current amplitude of the GluA2Q<sub>flip</sub> receptors, using a laser-pulse photolysis and a rapid solution flow technique. We further investigated whether BDZ-*f* interacts with two other known binding sites on GluA2Q<sub>flip</sub>, which we reported earlier;<sup>1,2</sup> one site is where GYKI 52466 binds, and the other is where BDZ-2 binds. Our findings establish that (i) BDZ-*f* is a noncompetitive inhibitor with a slight preference for the closed-channel over the open-channel state, (ii) BDZ-*f* is a nonselective inhibitor for the flip and flop variants of GluA2Q because it inhibits both equally well, and (iii) like other 2,3-benzodiazepine compounds we have characterized,<sup>1,2</sup> BDZ-*f* inhibits GluA2Q<sub>flip</sub> by forming an initial, loose intermediate that is still partially conducting, yet this intermediate rapidly isomerizes into a tighter, fully inhibitory receptor–inhibitor complex, and (iv) BDZ-*f* binds to the same noncompetitive site as GYKI 52466 does on the GluA2Q<sub>flip</sub> receptor. This site, however, is not the same site where BDZ-2 binds.

BDZ-*f* is synthesized as a structural derivative of the parent template, i.e., 2,3-benzodiazepine ring structure or GYKI 52466, the prototypic 2,3-benzodiazepine compound (Figure 1).<sup>25,26</sup> The results from the present investigation establish that BDZ-*f* is a better inhibitor than GYKI 52466. Defined by the overall inhibition constant or  $\bar{K}_i$  associated with the open-channel state of GluA2Q<sub>flip</sub> (Table 1), BDZ-*f* is 6-fold stronger than GYKI 52466 ( $\bar{K}_i$  is 5.4  $\mu$ M for BDZ-*f* and 30  $\mu$ M for GYKI 52466; see Table 1). For the closed-channel state, BDZ-*f* is 4-fold better than GYKI 52466 ( $K_i$  is 3.8  $\mu$ M for BDZ-*f* and 14  $\mu$ M for GYKI 52466).

The higher potency of BDZ-*f*, compared with GYKI 52466, can be best accounted for on the basis of the structure–activity relationship. (i) The finding that BDZ-*f* and GYKI 52466 bind to the same noncompetitive site on the GluA2Q<sub>flip</sub> receptor (Figure 6A) suggests that the addition of an *N*-3 methylcarbamoyl group on the diazepine ring of GYKI 52466 improves potency without changing the site of binding of the new compound, i.e., BDZ-*f*. (ii) The higher potency of BDZ-*f* seems to be realized even at the first step involving the formation of the initial, partially inhibitory receptor:inhibitor intermediate (Figure 4). Specifically, the GluA2Q<sub>flip</sub>:BDZ-*f* intermediate formed in the closed-channel state is about 3-fold more inhibitory than the GYKI 52466:receptor counterpart ( $K_i^* = 22 \mu$ M for

BDZ-*f* and 61  $\mu$ M for GYKI 52466; see Table 1). The GluA2Q<sub>flip</sub>:BDZ-*f* intermediate formed in the open-channel state is 6-fold more inhibitory than the GYKI 52466:receptor intermediate ( $\bar{K}_i^*$  is 20  $\mu$ M for BDZ-*f* but 128  $\mu$ M for GYKI 52466, respectively). This comparison suggests that the addition of an *N*-3 methylcarbamoyl group to the 2,3-benzodiazepine ring of GYKI 52466 makes BDZ-*f* more adaptable for binding to and interacting with the same noncompetitive site. (iii) GYKI 52466 shows a 2-fold selectivity for the closed-channel over the open-channel state (i.e., the inhibition constants for the closed-channel and the open-channel states are 14 and 30  $\mu$ M, respectively).<sup>2</sup> Addition of an *N*-3 methylcarbamoyl group to form BDZ-*f* reduced that selectivity (i.e., the inhibition constants for the closed- and open-channel states were  $\sim$ 3.8 and  $\sim$ 5.4  $\mu$ M, respectively) but strengthened the overall inhibition constants for both the open- and closed-channel states.

Addition of an *N*-3 methylcarbamoyl group to the diazepine ring of GYKI 52466, resulting in BDZ-*f*, clearly yields a more potent inhibitor. This result stands in stark contrast with addition of the same *N*-3 methylcarbamoyl group to the diazepine ring of BDZ-2, thus resulting in a new compound termed BDZ-3 (Figure S1).<sup>1</sup> BDZ-3, like BDZ-2, has a  $\epsilon$ -lactam structure (Figure S1) in which a 4-carbonyl group replaces the 4-methyl group as in the azomethine ring structure of GYKI 52466. However, BDZ-3, which contains an *N*-3 methylcarbamoyl group, is a weaker inhibitor than BDZ-2 although the mechanism of action of BDZ-3 and the binding site are the same as those of BDZ-2. These results suggest that the functional impact of the addition of an *N*-3 methylcarbamoyl group depends on the nature of the C-4 group. The addition of the *N*-3 methylcarbamoyl group to the azomethine structure of the diazepine ring gives rise to a stronger inhibitor (such as BDZ-*f* vs GYKI 52466). In contrast, the addition of the same group to the  $\epsilon$ -lactam structure of the diazepine ring yields a weaker inhibitor (BDZ-3 vs BDZ-2) for GluA2Q<sub>flip</sub><sup>1</sup> and is therefore undesirable. In either case, the addition of an *N*-3 methylcarbamoyl group does not change the destination of the resulting compound on the receptor; namely, the new compound continues to bind to the same site. On the contrary, the substitution of the azomethine group on the diazepine ring with a  $\epsilon$ -lactam structure changes the binding site for these noncompetitive inhibitors.<sup>2</sup> Consistent with this feature of the structure–activity relationship, BDZ-*f* competes at the same noncompetitive site with GYKI 52466, but this site is not the same one to which BDZ-2 binds (Figure 6B). Thus, BDZ-2 and BDZ-*f* can independently bind to their respective sites on GluA2Q<sub>flip</sub>, thereby producing greater inhibition when the two are used together.

In the present study, we have shown that the addition of an *N*-3 methylcarbamoyl group to the diazepine ring with the azomethine feature (i.e., GYKI 52466) is what makes BDZ-*f* better than the original GYKI 52466. Further studies are needed to determine whether this structural feature and/or addition of other types of functional groups at the *N*-3 position imparts the same functionality, namely, a more potent effect but without changing the site of binding. Other factors, which include shape and stereochemical arrangement of the same size, may be also involved in defining the functionality of the resulting compounds and should also be explored. In addition, the results from this study suggest the possibility of making new 2,3-benzodiazepine derivatives with different properties, such as water solubility, as well as the possibility of converting new

compounds into potentially useful photolabels for site mapping without losing the biological activity and site specificity.

## APPENDIX

The channel-opening kinetic process, observed in a laser-pulse photolysis measurement, followed a single-exponential rate expression, in eq 1, for ~95% of the rise time.

$$I_t = I_{\max}(1 - e^{-k_{\text{obs}}t}) \quad (1)$$

In eq 1,  $I_t$  represents the current amplitude at time  $t$  and  $I_{\max}$  the maximum current amplitude. From eq 1, an observed rate constant,  $k_{\text{obs}}$ , can be calculated. By the upper scheme in Figure 4, which represents channel opening (or without inhibitor bound),  $k_{\text{obs}}$  can be expressed in eq 2. In deriving eq 2, it is assumed that the ligand-binding rate is fast relative to the channel-opening rate. This assumption is supported by experimental result for GluA2Q<sub>flip</sub> channel opening, which we reported earlier and which we discussed in the text.

$$k_{\text{obs}} = k_{\text{cl}} + k_{\text{op}} \left( \frac{L}{L + K_1} \right)^2 \quad (2)$$

When the channel-opening rate was inhibited noncompetitively (as in Figure 4), the expression for the observed first-order rate constant was given by eq 3, where only one rate was observable. (This rate is assigned to the first step, corresponding to the formation of the initial inhibitor–receptor intermediate.) As such, the effect of an inhibitor on the channel-closing rate constant,  $k_{\text{cl}}$ , was determined using eq 4, where the inhibition constant associated with the open-channel state ( $\bar{K}_1$ ) could be estimated (at low ligand concentration: see text for further explanation). At higher ligand concentrations, the difference between  $k_{\text{obs}}$  and  $k_{\text{cl}}$  was determined, giving rise to the effect of an inhibitor on  $k_{\text{op}}$ , as shown in eq 5.

$$k_{\text{obs}} = k_{\text{cl}} \left( \frac{\bar{K}_1}{\bar{K}_1 + I} \right) + k_{\text{op}} \left( \frac{L}{L + K_1} \right)^2 \left( \frac{K_1}{K_1 + I} \right) \quad (3)$$

$$\frac{1}{k_{\text{obs}}} = \frac{1}{k_{\text{cl}}} + \frac{1}{k_{\text{cl}}} \frac{I}{\bar{K}_1} \quad (4)$$

$$(k_{\text{obs}} - k'_{\text{cl}})^{-1} = [k_{\text{op}}L / (L + K_1)^2]^{-1} (1 + I / K_1) \quad (5)$$

The experimental design of measuring the effect of an inhibitor on the current amplitude ( $A$ ) to determine the inhibition constant for both the open- and closed-channel states is as follows. At low glutamate concentrations (i.e.,  $L \ll K_1$ ), the majority of the receptor were in the closed-channel state (see Figure 4; defined as the unliganded, singly and doubly liganded forms). Under this condition, the inhibition constant for the closed-channel state was determined from the ratio of the amplitude according to eqs 6a and 6b. In contrast, the majority of the receptors were in the open-channel state at a saturating ligand concentration (i.e.,  $L \gg K_1$ ), and consequently, the inhibition constant for the open-channel state was measured. By using the two ligand concentrations that corresponded to ~4% and ~95% of the open-channel form, we determined whether the same compound inhibited the open- and closed-channel states differently. At those low and high ligand concentrations, the apparent inhibition constants obtained were considered pertinent to the closed- and open-channel states, respectively.

The ratio of the maximum current amplitudes in the absence,  $A$ , and presence,  $A_I$ , of an inhibitor was derived<sup>24</sup> and is shown in eq 6a.

$$\frac{A}{A_I} = 1 + I \frac{(\bar{A}L_2)_0}{K_I} \quad (6a)$$

where  $(\bar{A}L_2)_0$  represents the fraction of the open-channel form and is proportional to the current amplitude. In eq 6b, this fraction is expressed as a function of the fraction of all receptor forms.

$$\begin{aligned} (\bar{A}L_2)_0 &= \frac{\bar{A}L_2}{A + AL + AL_2 + \bar{A}L_2} \\ &= \frac{L^2}{L^2(1 + \Phi) + 2K_1L\Phi + K_1^2\Phi} \end{aligned} \quad (6b)$$

It should be noted that eqs 6a and 6b permitted the calculation of an inhibition constant at a defined agonist concentration. This is especially important for an inhibitor which shows differential selectivity for the open-channel over the closed-channel states or vice versa. In this case, the apparent inhibition constant,  $K_{I,\text{app}}$ , is dependent on the agonist concentration.

To determine whether BDZ-*f* and GYKI 52466, for instance, bound to the same site or two different sites (i.e., two mutually exclusive sites), the two inhibitors were used simultaneously to inhibit the channel activity. Specifically, the amplitude was used, similar to eqs 6a and 6b, to plot  $A/A_{I,P}$  vs one inhibitor concentration. Here, one inhibitor was represented as  $I$  in molar concentration while the other was  $P$ . Based on the assumption that one inhibitor bound per receptor and binding of inhibitor excluded the binding of the other (i.e., one-site model or  $A_I$  or  $A_P$  are allowed but not  $A_{I,P}$ ), the ratio of the current amplitude is given in eq 7.

$$\text{one-site model: } \frac{A}{A_{I,P}} = \left( 1 + \frac{P}{K_P} \right) + \frac{I}{K_I} \quad (7)$$

On the other hand, for a two-site model in which there was one site for  $I$  and another for  $P$  separately (i.e., both  $A_I$  and  $A_P$  and  $A_{I,P}$  are all allowed), the ratio of the current amplitude is given in eq 8.

$$\text{two-site model: } \frac{A}{A_{I,P}} = \left( 1 + \frac{P}{K_P} \right) + \left( 1 + \frac{P}{K_P} \right) \frac{I}{K_I} \quad (8)$$

## ASSOCIATED CONTENT

### Supporting Information

Comparison of the absolute current amplitude of the desensitizing phase and the nondesensitizing phase from the same cell (Table S1) and the chemical structures of BDZ-2 [1-(4-aminophenyl)-3,5-dihydro-7,8-methylenedioxy-4H-2,3-benzodiazepin-4-one] and BDZ-3 [1-(4-aminophenyl)-3-methyl-carbamoyl-7,8-methylenedioxy-4H-2,3-benzodiazepin-4-one] (Figure S1). This material is available free of charge via the internet at <http://pubs.acs.org>.

## AUTHOR INFORMATION

### Corresponding Author

\*Tel: 518-591-8819. Fax: 518-442-3462. E-mail: [lniu@albany.edu](mailto:lniu@albany.edu).

## Present Address

<sup>†</sup>Department of Pharmacology & Physiology, UMDNJ—New Jersey Medical School.

## Funding

This work was supported by grants from NIH/NINDS (R01 NS060812) and the Muscular Dystrophy Association (to L.N.).

## ACKNOWLEDGMENTS

We thank Sandor Solyom from IVAX for generously providing the BDZ-*f* for this study.

## ABBREVIATIONS

AMPA,  $\alpha$ -amino-3-hydroxy-5-methyl-4-isoxazolepropionic acid; BDZ, 2,3-benzodiazepine compounds; GYKI 52466, 1-(4-aminophenyl)-4-methyl-7,8-methylenedioxy-5H-2,3-benzodiazepine; BDZ-*f*, GYKI 53784, LY 303070, (–)-1-(4-aminophenyl)-4-methyl-7,8-methylenedioxy-4,5-dihydro-3-methylcarbamoyl-2,3-benzodiazepine; HEK-293 cells, human embryonic kidney 293 cells.

## REFERENCES

- (1) Ritz, M., Micale, N., Grasso, S., and Niu, L. (2008) Mechanism of inhibition of the GluR2 AMPA receptor channel opening by 2,3-benzodiazepine derivatives. *Biochemistry* 47, 1061–1069.
- (2) Ritz, M., Wang, C. Z., Micale, N., Ettari, R., and Niu, L. (2011) Mechanism of Inhibition of the GluA2 AMPA Receptor Channel Opening: the Role of 4-Methyl versus 4-Carbonyl Group on the Diazepine Ring of 2,3-Benzodiazepine Derivatives. *ACS Chem. Neurosci.*, in press.
- (3) Davies, J., and Watkins, J. C. (1981) Differentiation of kainate and quisqualate receptors in the cat spinal cord by selective antagonism with gamma-D( and L)-glutamylglycine. *Brain Res.* 206, 172–177.
- (4) Dingledine, R., Borges, K., Bowie, D., and Traynelis, S. F. (1999) The glutamate receptor ion channels. *Pharmacol. Rev.* 51, 7–61.
- (5) Palmer, C. L., Cotton, L., and Henley, J. M. (2005) The molecular pharmacology and cell biology of alpha-amino-3-hydroxy-5-methyl-4-isoxazolepropionic acid receptors. *Pharmacol. Rev.* 57, 253–277.
- (6) Cull-Candy, S., Kelly, L., and Farrant, M. (2006) Regulation of Ca<sup>2+</sup>-permeable AMPA receptors: synaptic plasticity and beyond. *Curr. Opin. Neurobiol.* 16, 288–297.
- (7) Liu, S. J., and Zukin, R. S. (2007) Ca<sup>2+</sup>-permeable AMPA receptors in synaptic plasticity and neuronal death. *Trends Neurosci.* 30, 126–134.
- (8) Hume, R. I., Dingledine, R., and Heinemann, S. F. (1991) Identification of a site in glutamate receptor subunits that controls calcium permeability. *Science* 253, 1028–1031.
- (9) Zappala, M., Grasso, S., Micale, N., Polimeni, S., and De Micheli, C. (2001) Synthesis and structure-activity relationships of 2,3-benzodiazepines as AMPA receptor antagonists. *Mini-Rev. Med. Chem.* 1, 243–253.
- (10) Solyom, S., and Tarnawa, I. (2002) Non-competitive AMPA antagonists of 2,3-benzodiazepine type. *Curr. Pharm. Des.* 8, 913–939.
- (11) Tarnawa, I., Farkas, S., Berzsenyi, P., Pataki, A., and Andras, F. (1989) Electrophysiological studies with a 2,3-benzodiazepine muscle relaxant: GYKI 52466. *Eur. J. Pharmacol.* 167, 193–199.
- (12) Li, G., Pei, W., and Niu, L. (2003) Channel-opening kinetics of GluR2Q(flip) AMPA receptor: a laser-pulse photolysis study. *Biochemistry* 42, 12358–12366.
- (13) Wieboldt, R., Gee, K. R., Niu, L., Ramesh, D., Carpenter, B. K., and Hess, G. P. (1994) Photolabile precursors of glutamate: synthesis, photochemical properties, and activation of glutamate receptors on a microsecond time scale. *Proc. Natl. Acad. Sci. U. S. A.* 91, 8752–8756.
- (14) Li, G., Oswald, R. E., and Niu, L. (2003) Channel opening kinetics of GluR6 kainate receptor. *Biochemistry* 42, 12367–12375.
- (15) Chen, C., and Okayama, H. (1987) High-efficiency transfection of mammalian cells by plasmid DNA. *Mol. Cell. Biol.* 7, 2745–2752.
- (16) Huang, Z., Li, G., Pei, W., Sosa, L. A., and Niu, L. (2005) Enhancing protein expression in single HEK 293 cells. *J. Neurosci. Methods* 142, 159–166.
- (17) Udgaonkar, J. B., and Hess, G. P. (1987) Chemical kinetic measurements of a mammalian acetylcholine receptor by a fast-reaction technique. *Proc. Natl. Acad. Sci. U. S. A.* 84, 8758–8762.
- (18) Li, G., Niu, L. (2004) How fast does the GluR1Q(flip) channel open? *J. Biol. Chem.* 279, 3990–3997. Epub 2003 Nov 3910.
- (19) Sommer, B., Keinänen, K., Verdoorn, T. A., Wisden, W., Burnashev, N., Herb, A., Kohler, M., Takagi, T., Sakmann, B., and Seeburg, P. H. (1990) Flip and flop: a cell-specific functional switch in glutamate-operated channels of the CNS. *Science* 249, 1580–1585.
- (20) Mayer, M. L., and Vyklicky, L. Jr. (1989) Concanavalin A selectively reduces desensitization of mammalian neuronal quisqualate receptors. *Proc. Natl. Acad. Sci. U. S. A.* 86, 1411–1415.
- (21) Koike, M., Tsukada, S., Tsuzuki, K., Kijima, H., and Ozawa, S. (2000) Regulation of kinetic properties of GluR2 AMPA receptor channels by alternative splicing. *J. Neurosci.* 20, 2166–2174.
- (22) Lee, C. J., Labrakakis, C., Joseph, D. J., and Macdermott, A. B. (2004) Functional similarities and differences of AMPA and kainate receptors expressed by cultured rat sensory neurons. *Neuroscience* 129, 35–48.
- (23) Brorson, J. R., Manzolillo, P. A., Gibbons, S. J., and Miller, R. J. (1995) AMPA receptor desensitization predicts the selective vulnerability of cerebellar Purkinje cells to excitotoxicity. *J. Neurosci.* 15, 4515–4524.
- (24) Pei, W., Huang, Z., Wang, C., Han, Y., Park, J. S., and Niu, L. (2009) Flip and flop: a molecular determinant for AMPA receptor channel opening. *Biochemistry* 48, 3767–3777.
- (25) Lodge, D., Bond, A., O'Neill, M. J., Hicks, C. A., and Jones, M. G. (1996) Stereoselective effects of 2,3-benzodiazepines in vivo: electrophysiology and neuroprotection studies. *Neuropharmacology* 35, 1681–1688.
- (26) Bleakman, D., Ballyk, B. A., Schoepp, D. D., Palmer, A. J., Bath, C. P., Sharpe, E. F., Woolley, M. L., Bufton, H. R., Kamboj, R. K., Tarnawa, I., and Lodge, D. (1996) Activity of 2,3-benzodiazepines at native rat and recombinant human glutamate receptors in vitro: stereospecificity and selectivity profiles. *Neuropharmacology* 35, 1689–1702.